Interior Permanent Magnet Synchronous Machine Drive Powered by Fuel Cell for Automotive Applications

Claudio Nevoloso, Nicola Campagna, Massimo Caruso, Vincenzo Castiglia, Antonino Oscar Di Tommaso and Rosario Miceli, *IEEE Member*
Department of Engineering, University of Palermo
Palermo, Italy
email: claudio.nevoloso@unipa.it

***Abstract*—Electric vehicles represent an optimal solution for the reduction of pollution in urban areas. In particular, the Fuel Cell (FC) technology is a promising solution especially for its charging times and zero CO_2 direct emissions. The paper addresses the design and performance study of an Interior Permanent Magnet Synchronous Machine (IPMSM) drive powered by fuel cell for automotive applications. The IPMSM drive is powered by the use of 5,5 kW FC unit and it is composed of two DC-DC power converters and one inverter. In detail, a test bench has been carried out for the evaluation of the performances of each IPMSM drive conversion stage. Moreover, in order to simulate automotive working conditions the European Standard Urban Driving Cycle (UDC) test is used in order to evaluate the performances of the electric drive. The experimental results are discussed in order to highlight the benefits and the adoption of possible solutions in order to improve the overall performances of the electric drive.**

Keywords— Electric vehicles, hydrogen fuel cell, IPMSM drive.

I. Introduction

Climate changes and global warming issues are becoming fundamental for humanity since their effects will have a huge impact on the life quality of future generations. In the last decade, the environmental pollution topic has become a problem much discussed by the social and political communities since it generates economic and social costs. The overall transport section generates 30 % of total EU fuel emission and a doubling of energy consumption has been detected in 2018 respect to 2010 resulting in an increase in CO_2 emissions [1]. In this context, a possible solution in order to reduce environmental pollution is the adoption of hybrid and electric vehicles.

In the last few years, the scientific communities focused their efforts in the research of high performances drive technologies [2] and innovative energy storage systems [7]. The commercial hybrid and electric vehicles technologies are continuously rising [14]-[22] and they are based on the use of batteries and their main disadvantages are the low power density, long charge times and short life span. Moreover, the manufacturing of batteries requires chemical materials whose manufacture is a source of indirect CO_2 emissions.

The hydrogen FC technologies are interesting and alternative energy source devices that can be employed in automotive applications. In detail, an interesting study demonstrates that if the hydrogen is produced from natural gas or hydrocarbons fuel the CO_2 emissions can be reduced by 50% respect to conventional internal combustion engine (ICE) while when the hydrogen is produced by the use of renewable energy source the CO_2 emissions can be reduced by 90% [25]. In particular, the use of Polymer Electrolyte Membrane Fuel Cell (PEMFC) for automotive applications has been widely discussed by scientific literature and several improvements have been registered. In detail, several studies investigate and discuss the adoption of fuel cell technology in several kinds of vehicles such as motorcycle [26], hybrid-electric pedal-assisted cycles [27], city bus [28] and light urban electric vehicle [30]. This FC topology employs pure hydrogen for the generation of electrical energy and not requires reforming with consequent saving of utility costs. The main drawbacks of PEMFC consist of lower energy density and non-linear behaviour in dynamic working conditions respect the batteries. Generally, the use of PEMFC for practical applications is coupled with the use of other energy sources like batteries and supercapacitors.

In this paper, a prototype of IPMSM electric drive powered by the fuel cell has been assembled in order to emulate the powertrain of an electric vehicle. This work addresses the study of the IPMSM electric drive performances supplied by the use of PEMFC. In detail, the study described here represents the basis for a more complex study that involves the use of other energy sources (batteries and supercapacitors) for the optimal use of the energy onboard an electric vehicle with consequents benefits in terms of static and dynamic performances. For this purpose, a flexible test bench has been set up and the speed profile of the UDC test has been used to driving the IPMSM drive and simulate typical automotive load conditions. In particular, several experimental tests have been carried out in order to evaluate the performances of IPMSM drive powered by fuel cell. The study conducted allowed to evaluate not only the overall efficiency of the system analyzed in dynamic conditions but even of each energy conversion stage.

The paper is structured as follows: Section II described the structure of the IPMSM drive powered by the fuel cell and its main components, Section III describes the test bench used for the experimental characterization and Section IV presents and discusses the experimental results.

II. Components of the IPMSM Drive Powered by Fuel Cell

Fig. 1 reports the schematic representation of IPMSM drive powered by the fuel cell.

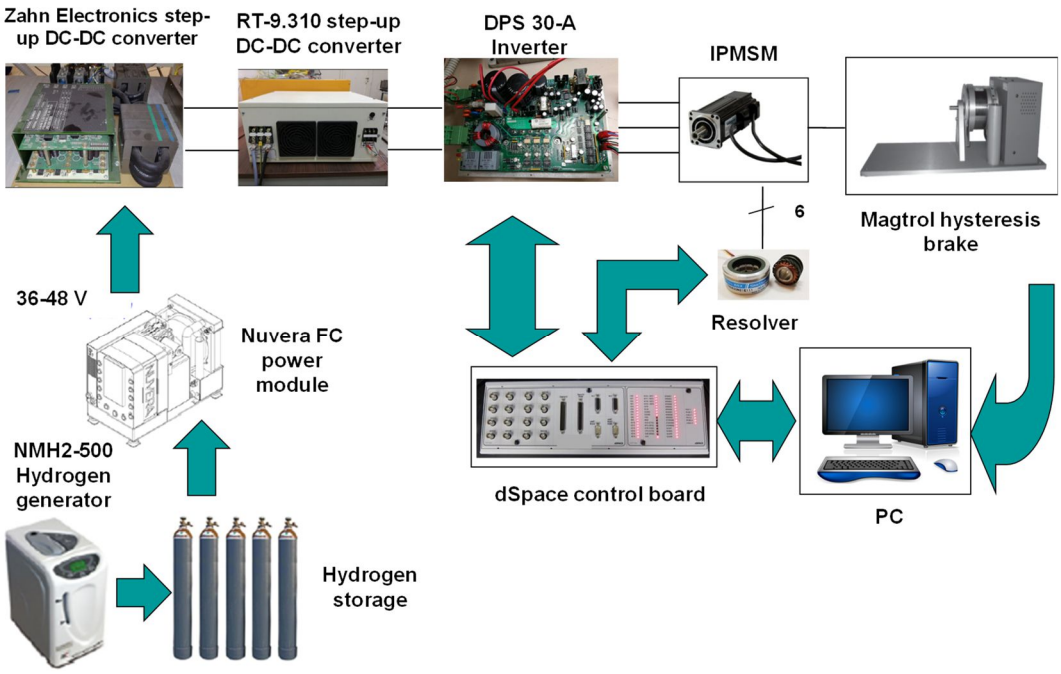

Fig. 1 Schematic representation of the IPMSM drive powered by the fuel cell.

In detail, a 5,5 kW FC Power Module composed of 40 cells produced by Nuvera is used. The hydrogen necessary for the operation of the Power Flow module is produced by using distilled water with conductivity less than 2 µS / cm. In detail, a generator of the DBS-Analytical Instruments NMH2-500 has been adopted. The hydrogen produced, subsequently is stored in 5 storage bottles of 40 litres at a pressure of 10 bar. A Teledyne Hastings 200 series flow meter is used in order monitoring the flow of hydrogen in the feed and it allows to samples the hydrogen flow time trend. The output voltage of FC Power Module is a function of the output current and, therefore, a step-up DC-DC converter (produced by Zahn Electronics) is employed in order to stabilize the output voltage at a value of 48 V.

The IPMSM drive is composed of:

- a DPS 30-A inverter (Automotion Inc.), whose nameplate data are summarized in Table I;
- a commercial 6 poles, three-phase IPMSM (Magnetic S.r.l., type BLQ-40, Italy) with interior Smco magnets, whose nameplate data are summarized in Table II;
- a Magtrol hysteresis brake (Model HD-715-8NA), connected to the shaft of the motor and used as a mechanical load for the IPMSM. The brake can be controlled in real-time through a digital dynamometer controller (Magtrol DSP6001) or with Labview® environment. The dynamometer controller provides the torque and speed signals that can be acquired with other acquisition systems;
- a PC with dSpace® based electrical drive user interface, which allows performing the real-time control of the proposed system.

In order to adapt the output DC voltage of the Zahn Electronics DC-DC power converter to the input DC voltage of the DPS 30-A DC-AC inverter, a further RT-9.310 step-up DC-DC converter is used. The main data of RT-9.310 step-up DC-DC converter are summarized in Table III.

- TABLE I DPS 30-A INVERTER NAMEPLATE DATA.

Parameter	*Value*
Rated DC voltage [V]	310
Phase current peak [A]	30
Phase current (rms) [A]	21
Output power peak [kW]	6.5
PWM frequency[kHz]	2-20

- TABLE II IPMSM NAMEPLATE DATA.

Parameter	*Value*
Voltage [V]	132
Current [A]	3.6
Rated mechanical speed [rpm]	4000
Nominal torque [Nm]	1.8

- TABLE III RT-9.310 DC-DC POWER CONVERTER NAMEPLATE DATA.

Parameter	*Value*
Rated input DC voltage [V]	48
Output DC voltage [V]	310
Rated power [kW]	3
Output power peak [kW]	7

III. TEST BENCH

In order to simulate the typical working condition of an electric drive used in automotive applications, the speed profile of the standard European Standard UDC test (Fig. 2) is considered to driving the IPMSM drive.

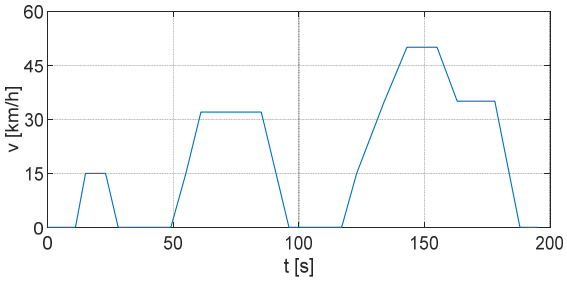

Fig. 2 UDC speed profile.

The speed profile of UDC test is scaled on the base of the rated speed of IPMSM. A Field Oriented Control (FOC) strategy, schematically reported in Fig. 3, has been experimentally implemented in dSpace® control board in order to control the IPMSM drive [28].

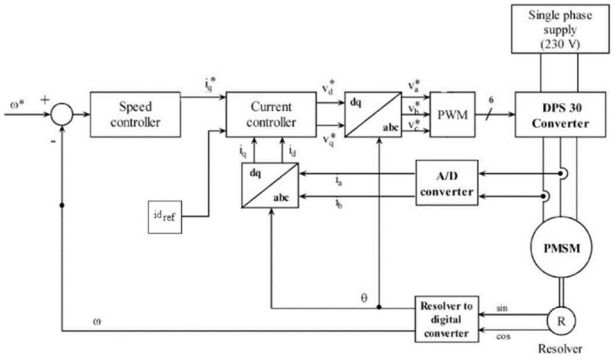

Fig. 3 Schematic representation of FOC strategy implemented in dSpace® control board.

The FOC presents an external closed-loop of the mechanical speed and two internal closed-loop of the dq-axis currents. The reference value of mechanical speed ω^* has been defined by the use of the lookup table where the speed profile of UDC test can be implemented.

For the design purpose of the test bench, the IPMSM drive powered by FC has been divided into two subsystems. The first subsystem includes the electricity generation from the FC Power Module with its electrical power conditioning components or Zahn Electronics step-up DC-DC converter. In detail, beyond the measurement of hydrogen flow, the input and output electrical quantities of Zahn Electronics step-up DC-DC converter are considered for the characterization of the first subsystem. The second subsystem includes the IPMSM electric drive and RT-9.310 step-up DC-DC converter. In this case, the input electrical quantities of DPS 30-A inverter and the output mechanical quantities of the IPMSM are considered in order to characterize the second subsystem. For each subsystem defined, below the measurement equipment adopted are described.

A. Measurement equipment of subsystem 1

For the characterization of subsystem 1, the National instruments modules and Labview programming environment have been chosen in order to have a flexible measurement system. The acquisition system consists of a NI cdaq-9172 chassis equipped with a NI9215 module for the acquisition of electrical quantities. The NI9215 module has four analog input channels, simultaneous sampling mode, sampling frequency f_s= 1.613−100 kS/s, ADC delta-sigma, 16-b resolution, and input ranges of ±10V. The voltage quantities are sensed by the use of a resistive divider. The measurement of current quantities are performed by the use of two Cropico precision shunt resistances of 0.1 Ω and nominal current equal to 22 A. The schematic representation of the measurement circuit is reported in Fig. 4.

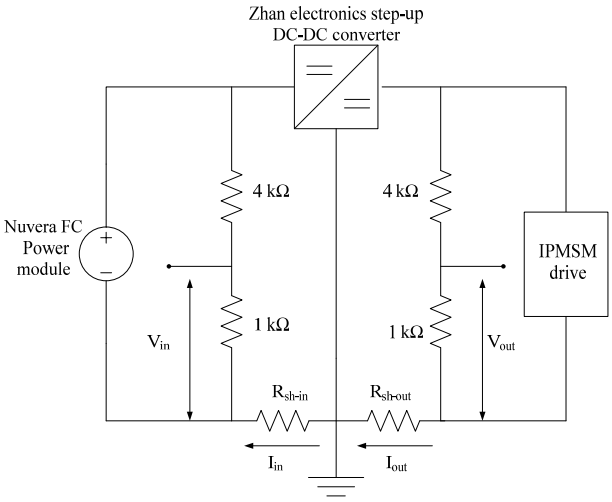

Fig. 4 Measurement circuit of the voltage quantities.

The acquisition of measurement signals is implemented in a virtual instrument on Labview® environment where the sample rate is imposed equal to 50 kS/s. Since the measurement must be synchronized with the applications of speed profile, the synchronization between the dSpace® control board of the IPMSM drive and the virtual instrument is necessary. For this purpose, a NI DAQ 9401 acquisition module has been used in order to acquire a trigger digital signal generated by the dSpace® control board. The NI DAQ 9401 acquisition module has the following features: eight digital input channels, 5 V/TTL signal level, simultaneous sampling mode, 100 ns update rate. From the acquired signals the input power and output power of Zahn Electronics step-up DC-DC converter are calculated.

B. Measurement equipment of subsystem 2

Also for subsystem 2, the National instruments modules and Labview® programming environment have been chosen. The acquisition system consists of a programmable data acquisition board NI cdaq-9172 equipped with several acquisition modules NI. In detail, two NI DAQ 9215 acquisition modules are used for the acquisition of the torque, speed and current signal. A NI DAQ 9225 acquisition module is used for the acquisition of the IPMSM drive input voltage. The NI DAQ 9225 has four analogue input channels, simultaneous sampling mode, sampling frequency f_s= 1.613−50 kS/s, ADC delta-sigma with analogue prefiltering (alias-free bandwidth of 0.453 f_s), 24-b resolution, and input ranges of ±300 V. The current is sensed by the use of a non-inductive Fluke A40B Precision AC Current Shunt of 0.04 Ω and nominal current equal to 20 A. Both the acquisition of measurement signals and the real-time control of load torque value of the hysteresis brake are implemented in one virtual instrument on Labview® environment where the sample rate is imposed equal to 50 kS/s. Even in this case, it is necessary the synchronization between the control board of the IPMSM drive and the virtual instrument. For this purpose, another NI DAQ 9401 acquisition module has been used in order to acquire a trigger digital signal generated by the dSpace® control board. From the acquired signals it is possible to calculate the input

electric power and the output mechanical power. The measurements were performed after the calibration of the dynamometer and by controlling the temperature and humidity of the test laboratory.

IV. Experimental Results

The IPMSM drive has been driven by the use of UDC speed profile. Furthermore, in order to evaluate the performances of the system under load working condition, a load torque profile has been applied by the use of Magtrol hysteresis brake. In detail, a 0.5 Nm constant value of load torque has been applied. The torque load profile has been defined according to the speed profile and it is applied during the time intervals where the speed is different than zero in order to avoid locked rotor working condition with consequently high values of absorbed current by the IPMSM drive. Moreover, in order to perform a filtering action and eliminate the presence of noise in the acquired quantities, an average of the samples acquired every 1 s was carried out. Fig. 5 reports the mechanical speed profile and load torque of IPMSM drive acquired during the experimental test.

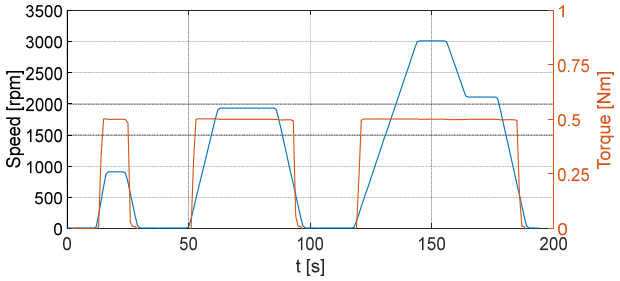

Fig. 5 IPMSM speed profile and its load torque.

From the acquired samples of input and output electrical quantities of the Zhan DC-DC converter, the instantaneous powers and consequently the active powers have been calculated. In detail, Fig. 6-Fig. 7 report the trends of the DC-DC conversion stage input active power and the DC-DC conversion stage output active power. The trends of input and output powers of the DC-DC conversion stage follow the UDC speed profile applied.

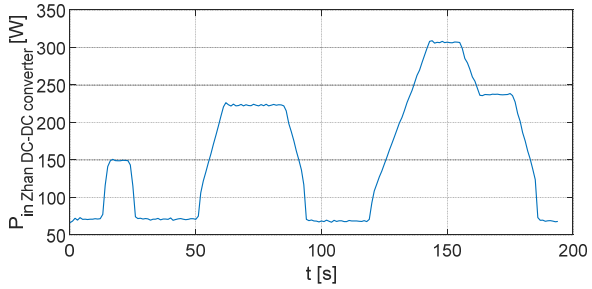

Fig. 6 Input power of Zhan DC-DC converter.

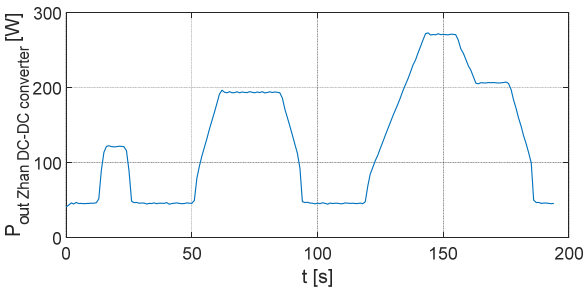

Fig. 7 Output power of Zhan DC-DC converter.

In the same way, the input and output active powers of IPMSM drive have been calculated from the samples of electrical quantities acquired by the use of measurement equipment of subsystem 2. Fig. 8-Fig. 9 report the trends of the IPMSM drive input active power and the IPMSM drive output active power. Even in this case, the trends of the active powers follow the speed profile of the UDC applied. In the trend of input electric power, some oscillations have been detected. This behaviour can be attributed to the dynamic behaviour of the IPMSM drive.

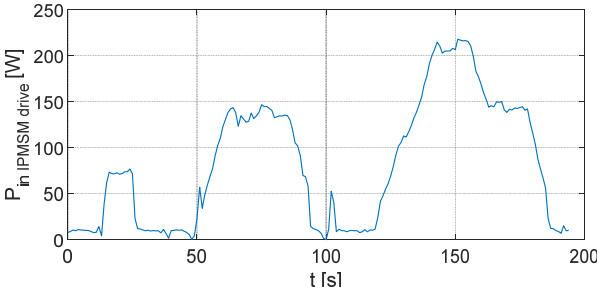

Fig. 8 Input electrical power of IPMSM drive.

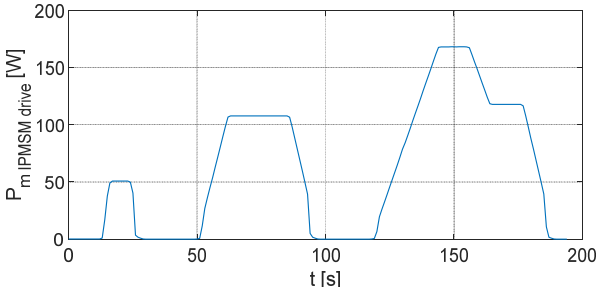

Fig. 9 Output mechanical power.

Starting from the values of active powers detected, the efficiency of each conversion stage has been calculated. For instance, Fig. 10-Fig. 12 report the efficiency of the Zhan DC-DC converter, the efficiency of the IPMSM drive and the total efficiency of the IPMSM drive powered by fuel cell, respectively.

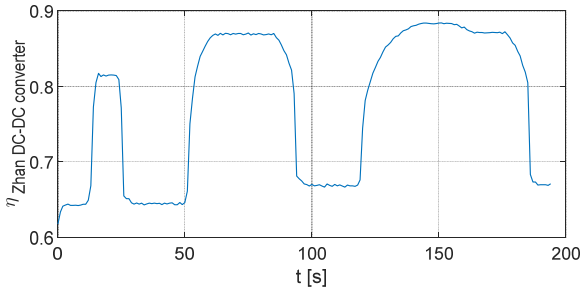

Fig. 10 Efficiency of the Zhan DC-DC converter.

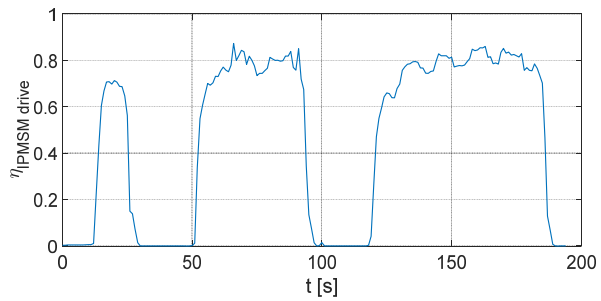

Fig. 11 Efficiency of the IPMSM drive.

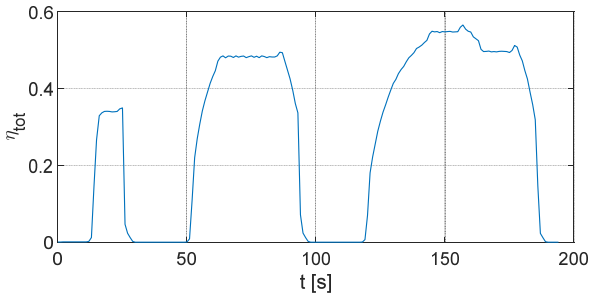

Fig. 12 Total efficiency of the IPMSM drive powered by the fuel cell.

In detail, the efficiency of DC-DC conversion stage presents high value when the electric drive works under load, while lower values of efficiency have been detected when the speed of the IPMSM drive is equal to zero. Similar behaviour has been detected for RT-9.310 DC-DC power converter but with slightly smaller values respect to the previous DC-DC conversion stage. The efficiency values of the IPMSM drive increases as the load increases in terms of speed and torque. This result can be attributed to the IPMSM efficiency typical behaviour that presents the highest values near to the nominal working condition. The overall efficiency of the IPMSM drive powered by the fuel cell presents values higher respect than typical efficiency values of the ICE power train. In detail, satisfactory values of the overall efficiency are obtained in correspondence of the highest working load condition. Therefore, from the experimental results obtained it is possible to assert that higher values of the efficiency can be obtained by employing DC-DC power converter with nominal power size optimized respect the nominal power of the electric drive. Furthermore, additional energy sources like battery and supercapacitors can be adopted in order to improve the dynamical behaviour of the IPMSM drive and obtain optimal use of the energy available by the fuel cell. Fig. 13 reports the trend of hydrogen flow detected during the UDC test.

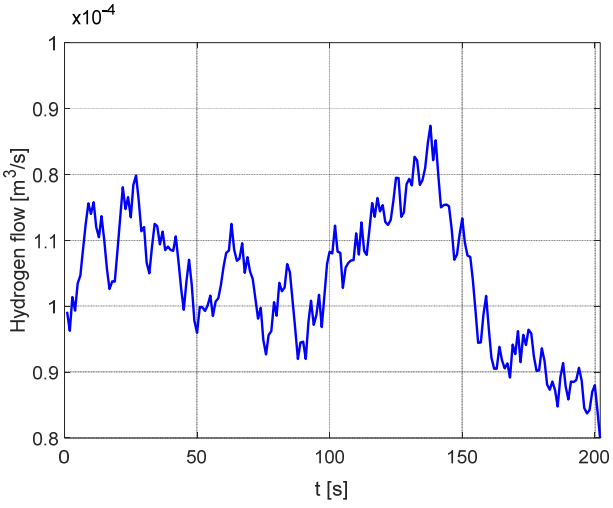

Fig. 13 Instantaneous hydrogen flow trend during the UDC test.

The hydrogen flow presents a peak value at the time instant of 140 s where the IPMSM drive works with the highest load condition. The instantaneous hydrogen flow has been integrated respect the time of the test and an overall hydrogen consumption of 0.179 m^3 has been detected.

V. Conclusions

The paper presents an experimental analysis on the performances of an IPMSM drive powered by fuel cell prototype. In detail, the IPMSM drive has been driving by the use of UDC speed profile in order to simulate the typical working load conditions of the automotive applications. The experimental investigations carried out allowed to detect the efficiency trends of each energy conversion stage of the IPMSM drive powered by fuel cell. In particular, the overall efficiency of the system analyzed can be improved by optimal sizing of the DC-DC conversion stages respect the nominal power of IPMSM drive. In future work, additional energy source, like batteries and supercapacitor, will be considered in order to improve the dynamic performances of the IPMSM drive powered by fuel cell and define a smart use of the energy available by the fuel cell.

Acknowledgment

This work was financially supported by PON R&I 2015-2020 “Propulsione e Sistemi Ibridi per velivoli ad ala fissa e rotante – PROSIB”, CUP no:B66C18000290005, by H2020-ECSEL-2017-1-IA-two-stage “first and european sic eightinches pilot line-REACTION”, by Prin 2017-Settore/Ambito di intervento: PE7 linea C -Advanced power-7 trains and -systems for full electric aircrafts, by PON R&I 2014-2020 -AIM (Attraction and International Mobility), project AIM1851228-1 and by ARS01_00459-PRJ-0052 ADAS+ “Sviluppo di tecnologie e sistemi avanzati per la sicurezza dell'auto mediante piattaforme ADAS”.

References

[1] G. Ala, V. Castiglia, G. Di Filippo, R. Miceli, P. Romano and F. Viola, "From electric mobility to hydrogen mobility: current state and possible future expansions," *2020 IEEE 20th Mediterranean Electrotechnical Conference (MELECON)*, Palermo, Italy, 2020, pp. 1-6, doi: 10.1109/MELECON48756.2020.9140482.

[2] B. Sarlioglu, C. T. Morris, D. Han and S. Li, "Driving Toward Accessibility: A Review of Technological Improvements for Electric Machines, Power Electronics, and Batteries for Electric and Hybrid Vehicles," in *IEEE Industry Applications Magazine*, vol. 23, no. 1, pp. 14-25, Jan.-Feb. 2017, doi: 10.1109/MIAS.2016.2600739.

[3] A. Stippich *et al*., "Key components of modular propulsion systems for next generation electric vehicles," in *CPSS Transactions on Power Electronics and Applications*, vol. 2, no. 4, pp. 249-258, December 2017, doi: 10.24295/CPSSTPEA.2017.00023.

[4] Dietz, A.; Di Tommaso, A.O.; Marignetti, F.; Miceli, R.; Nevoloso, C. Enhanced Flexible Algorithm for the Optimization of Slot Filling Factors in Electrical Machines.*Energies*2020,*13*, 1041.

[5] M. Caruso, A. O. Di Tommaso, M. Lombardo, R. Miceli, C. Nevoloso and C. Spataro, "Maximum Torque Per Ampere control algorithm for low saliency ratio interior permanent magnet synchronous motors," *2017 IEEE 6th International Conference on Renewable Energy Research and Applications (ICRERA)*, San Diego, CA, 2017, pp. 1186-1191, doi: 10.1109/ICRERA.2017.8191241.

[6] Caruso, M., Di Tommaso, A. O., Miceli, R., Nevoloso, C., Spataro, C., & Trapanese, M. (2019). Maximum torque per ampere control strategy for low-saliency ratio IPMSMs. *International Journal of Renewable Energy Research*, 9(1), 374-383.

[7] Tran, D.D.; Vafaeipour, M.; El Baghdadi, M.; Barrero, R.; Van Mierlo, J.; Hegazy, O. Thorough state-of-the-art analysis of electric and hybrid vehicle powertrains: Topologies and integrated energy management strategies. Renew. Syst. Energ. Rev. 2020, 119, 109596.

[8] A. Khaligh and Z. Li, "Battery, Ultracapacitor, Fuel Cell, and Hybrid Energy Storage Systems for Electric, Hybrid Electric, Fuel Cell, and Plug-In Hybrid Electric Vehicles: State of the Art," in *IEEE Transactions on Vehicular Technology*, vol. 59, no. 6, pp. 2806-2814, July 2010, doi: 10.1109/TVT.2010.2047877.

[9] M. Carignano, V. Roda, R. Costa-Castelló, L. Valiño, A. Lozano and F. Barreras, "Assessment of Energy Management in a Fuel Cell/Battery Hybrid Vehicle," in *IEEE Access*, vol. 7, pp. 16110-16122, 2019, doi: 10.1109/ACCESS.2018.2889738.

[10] Viola, F., Romano, P., Miceli, R., Spataro, C., Schettino, G., Fanto, F. Economic benefits of the use of a PV plants reconfiguration systems (2015) 2015 International Conference on Renewable Energy Research and Applications, ICRERA 2015, art. no. 7418687, pp. 1654-1658.

[11] Caruso, M., Cipriani, G., Di Dio, V., Miceli, R., Nevoloso, C. Experimental characterization and comparison of TLIM performances with different primary winding connections (2017) Electric Power Systems Research, 146, pp. 198-205.

[12] Viola, F., Romano, P., Miceli, R., Spataro, C., Schettino, G. Survey on power increase of power by employment of PV reconfigurator (2015) 2015 International Conference on Renewable Energy Research and Applications, ICRERA 2015, art. no. 7418689, pp. 1665-1668.

[13] Livreri, P., Caruso, M., Castiglia, V., Pellitteri, F., Schettino, G. Dynamic reconfiguration of electrical connections for partially shaded PV modules: Technical and economical performances of an Arduino-based prototype (2018) International Journal of Renewable Energy Research, 8 (1), pp. 336-344.

[14] Caruso, M., Di Tommaso, A.O., Genduso, F., Miceli, R., Galluzzo, G.R., 'A General Mathematical Formulation for the Determination of Differential Leakage Factors in Electrical Machines with Symmetrical and Asymmetrical Full or Dead-Coil Multiphase Windings', (2018) IEEE Transactions on Industry Applications, 54 (6), art. no. 8413120, pp. 5930-5940.

[15] L. Schirone, M. Macellari, F. Pellitteri, "Predictive dead time controller for GaN-based boost converters", *Power Electron.*, vol. 10, no. 4, pp. 421-428, 2017.

[16] Damiano A., Porru M., Salimbeni A., Serpi, A., Castiglia V., Di Tommaso A.O., Miceli R., Schettino G., Batteries for Aerospace: A Brief Review, (2018) 110th AEIT International Annual Conference, AEIT 2018.

[17] Schettino G., Castiglia V., Genduso F., Livreri P., Miceli R., Romano P., Viola F., Simulation of a single-phase five-level cascaded H-Bridge inverter with multicarrier SPWM B-Spline based modulation techniques, (2017) 12th International Conference on Ecological Vehicles and Renewable Energies, EVER 2017.

[18] Acciari, G., Caruso, M., Miceli, R., Riggi, L., Romano, P., Schettino, G., Viola, F. Piezoelectric Rainfall Energy Harvester Performance by an Advanced Arduino-Based Measuring System (2018) IEEE Transactions on Industry Applications, 54 (1), art. no. 8036268, pp. 458-468.

[19] Schettino G., Ala G., Caruso M., Castiglia V., Pellitteri F., Trapanese M., Viola F., Miceli R., "Experimental study on B-spline-based modulation schemes applied in multilevel inverters for electric drive applications", (2019) Energies.

[20] Caruso, M., Di Tommaso, A.O., Imburgia, A., Longo, M., Miceli, R., Romano, P., Salvo, G., Schettino, G., Spataro, C., Viola, F. Economic evaluation of PV system for EV charging stations: Comparison between matching maximum orientation and storage system employment (2017) 2016 IEEE International Conference on Renewable Energy Research and Applications, ICRERA 2016, art. no. 7884519, pp. 1179-1184.

[21] Viola, F., Romano, P., Miceli, R., Spataro, C., Schettino, G., 'Technical and economical evaluation on the use of reconfiguration systems in some EU countries for PV plants', (2017) IEEE Transactions on Industry Applications, 53 (2), art. no. 7736973, pp. 1308-1315.

[22] Castiglia, V., Di Noia, L., Livreri, P., Miceli, R., Nevoloso, C., Pellitteri, F., Viola, F., 'An efficient wireless power transfer prototype for electrical vehicles', 2017 6th International Conference on Renewable Energy Research and Applications, ICRERA 2017, 2017-January, pp. 1215-1220.

[23] H. Chu, X. Qu, S. Wong and C. K. Tse, "Design of an IPT Battery Charger with Double-sided LCC Compensation," *2018 IEEE Energy Conversion Congress and Exposition (ECCE)*, Portland, OR, 2018, pp. 1184-1189.

[24] N. Campagna, V. Castiglia, R. Miceli and F. Pellitteri, "A Bidirectional IPT system for Electrical Bicycle Contactless Energy Transfer," *2019 8th International Conference on Renewable Energy Research and Applications (ICRERA)*, Brasov, Romania, 2019, pp. 1063-1068.

[25] F. Viola, D. Zaninelli, G. Ala, G. Schettino, V. Castiglia and R. Miceli, "Forecasting the Diffusion of Hydrogen EV Refuelling Infrastructures in Italy," *2019 Fourteenth International Conference on Ecological Vehicles and Renewable Energies (EVER)*, Monte-Carlo, Monaco, 2019, pp. 1-5, doi: 10.1109/EVER.2019.8813602.

[26] J. D. Weigl, "Fuel cell triple hybrid drive train for motorcycle," *2014 Ninth International Conference on Ecological Vehicles and Renewable Energies (EVER)*, Monte-Carlo, 2014, pp. 1-5, doi: 10.1109/EVER.2014.6844118.

[27] N. Campagna, A. O. Di Tommaso, F. Genduso, R. Miceli, F. M. Raimondi and G. R. Galluzzo, "Experimental characterization of a proton exchange membrane fuel-cell for hybrid electric pedal assisted cycles," *2017 IEEE 6th International Conference on Renewable Energy Research and Applications (ICRERA)*, San Diego, CA, 2017, pp. 1210-1214, doi: 10.1109/ICRERA.2017.8191245.

[28] Caruso, M., Di Tommaso, A.O., Miceli, R., Nevoloso, C., Spataro, C., Viola, F., Comparison of three control drive systems for interior permanent magnet synchronous motors, (2017) 22nd IMEKO TC4 International Symposium and 20th International Workshop on ADC Modelling and Testing 2017: Supporting World Development Through Electrical and Electronic Measurements, 2017-September.

[29] G. D'Ovidio, C. Masciovecchio and N. Rotondale, "City bus powered by hydrogen fuel cell and flywheel energy storage system," *2014 IEEE International Electric Vehicle Conference (IEVC)*, Florence, 2014, pp. 1-5, doi: 10.1109/IEVC.2014.7056107.

[30] F. Marignetti, D. D'Aguanno, R. Arcese and S. Ivagnes, "Design of a drivetrain for a light urban electric vehicle powered by fuel cells," *2015 IEEE 1st International Forum on Research and Technologies for Society and Industry Leveraging a better tomorrow (RTSI)*, Turin, 2015, pp. 433-438, doi: 10.1109/RTSI.2015.7325136.